Low temperature heat capacity of the system "silica gel–calcium chloride–water"

Yuri I. Aristov · Yulia A. Kovalevskaya ·
Michael M. Tokarev · Igor E. Paukov

Abstract Heat capacity was measured for two composite systems based on silica gel KSK and calcium chloride confined to its pores. One corresponds to an anhydrous state, while another contains water bound with the salt to give the composition of $CaCl_2 \cdot 2.04H_2O$. The measurements were performed in the temperature range of 6–300 K with a vacuum adiabatic calorimeter. The smoothed experimental curves $C_p(T)$ were used for calculating the calorimetric entropy and the enthalpy increment for both studied systems as well as the effective heat capacity associated only with water in the hydrated composite. The heat capacities $C_p(298.15 \text{ K})$ of both composites were compared with those calculated as a linear addition of the heat capacities of silica gel and bulk calcium chloride (or its dihydrate) with appropriate weight coefficients.

Keywords Calcium chloride dihydrate · Low temperature heat capacity · Pore-size effect · Silica gel

Introduction

The heat capacity C_p is a fundamental property of any individual substance. Its measurement in a wide temperature range from low temperatures allows determination of other important thermodynamic parameters, e.g., the calorimetric entropy and enthalpy. In addition, experimental curves $C_p(T)$ give very useful information about phase transitions and characteristic temperatures at which different degrees of freedom are liberated. This article is addressed to experimental measurement of the heat capacity of a complex system which consists of two components of comparable weight fractions, namely, a silica gel KSK and calcium chloride confined to its pores [1]. The main motivation was to obtain for this composite the fundamental parameters mentioned above, thus, creating a base for thermodynamic calculations for tentative applications of this material in anhydrous and hydrated states [2]. In addition, we tried to get information for highlighting a question, whether the confined salt and its dihydrate have the same heat capacity as in bulk or any changes occur due to a small size of the confined phase or its interaction with the silica surface. Preparation of nanocomposites inside silica matrix and their thermodynamic properties are hot topics of modern materials science [3, 4]. The increase of the heat capacity [5, 6] as well as the decrease in the Debye temperature [7, 8] and the melting point [9] of nanoparticles as compared with the bulk values has been reported for many metals and alloys. On the other hand, these thermal parameters can either decrease or increase for nanoparticles embedded in a matrix [8, 10]. This substantially depends on the chemical interaction at interfaces between confined guest particles and the host matrix: e.g., if there is a strong "guest–host" bonding then the enhancement of the guest Debye temperature can be observed [10, 11].

Y. I. Aristov · M. M. Tokarev
Boreskov Institute of Catalysis SB RAS, Prospekt Lavrentieva 5,
Novosibirsk 630090, Russia
e-mail: aristov@catalysis.ru

Yu. A. Kovalevskaya · I. E. Paukov (✉)
Nikolaev Institute of Inorganic Chemistry SB RAS,
Prospekt Lavrentieva 3, Novosibirsk 630090, Russia
e-mail: paukov@niic.nsc.ru

Experimental

Sample preparation

The sample "$CaCl_2$ + silica gel" was synthesized by a dry impregnation of the low density silica gel KSK-1

(Reakhim, Russia) with a saturated aqueous solution of calcium chloride [1]. The specific surface of the silica gel was 260 $m^2 g^{-1}$, the pore volume was 1.0 $cm^3 g^{-1}$, and the average pore diameter was 15 nm as specified by the producer. The salt with the purity >99% of the "for analysis" grade was supplied by Merck and used as it was delivered. Silica grains of 0.5–1.0 mm in size were dried at 200 °C for 2 h to remove residual water. Dry silica grains were impregnated with a 40.4 wt% aqueous solution of calcium chloride. The volume of the solution was equal to the pore volume of the grains to ensure the location of the salt solution inside the pores. The solvent (water) was removed by heating sample up to 200 °C until its weight remained constant. The $CaCl_2$ content in the dry composite was 35.7 ± 0.1 mass%. The hydrated sample was prepared by equilibrating the dry sample with the water vapor at the relative pressure $P/P_o = 0.06$ obtained over a saturated NaOH solution [12]. The equilibrium water content was 10.57 mass% that corresponded to $N = 2.04 \pm 0.01$ mol of H_2O per 1 mol of $CaCl_2$.

The X-ray diffraction showed that the anhydrous sample consisted of amorphous silica gel and crystalline calcium chloride located inside the silica pores (the size of coherent scattering domains was about 15 nm). In the hydrated sample, the dihydrate of $CaCl_2$ was also situated inside the pores. The bulk salt or its dihydrate was not found.

Calorimetric measurements

The heat capacity C_p was measured with a low temperature vacuum adiabatic calorimeter described in [13]. Adiabatic conditions were maintained by automatic control. Measuring cell was made of nickel and had the volume of 6 cm^3 and the mass of 18.8 g. The mass of the anhydrous sample $CaCl_2–SiO_2$ (sample I) was 3.4140 g, while that of the hydrated sample $H_2O–CaCl_2–SiO_2$ (sample II) was 3.6869 g. The heat capacity was measured in a wide temperature range of 6–303 K in 65 and 63 calorimetric experiments for samples I and II, respectively. To improve the heat exchange during the calorimetric measurements, gaseous helium was passed into the calorimeter at the pressure 1.1×10^4 and 2.0×10^4 Pa for samples I and II, respectively. As the empty calorimetric ampoule was calibrated at lesser pressure of helium (1.3×10^3 Pa), the correction for the heat capacity of "extra" helium was made. It was equal to few tenths of a percent at 15 K and decreased quickly at higher temperature.

As the samples could quickly suck water from the atmosphere, special experiments were carried out to evaluate the mass of water absorbed during the sample loading inside the calorimeter. The loading time was minimized to 1–1.5 min, and the mass of water absorbed was ca. 0.26 mg that is 0.05% of total mass of water in the sample.

The accuracy of the heat capacity measurements was estimated taking into account a scatter of experimental points, calibration measurements of empty calorimetric ampoule, and measurements of a standard substance for calorimetry, namely, benzoic acid. The accuracy was estimated to be about 2% at 15 K, 1% at 25 K, and 0.4% at temperature from 40 to 300 K.
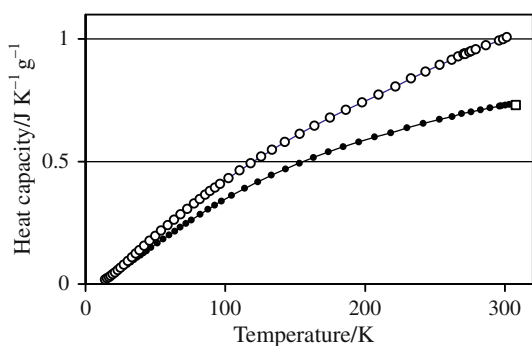
Results and discussion

Primary experimental data on the heat capacity of samples I and II are listed in Tables 1 and 2 and plotted in Fig. 1 as a function of temperature.

Table 1 Experimental heat capacity of the anhydrous composite "$CaCl_2$–silica gel" in J K^{-1} g^{-1}

T/K	C_p^o	T/K	C_p^o
15.26	0.02049	97.32	0.3380
16.32	0.02381	104.59	0.3609
16.72	0.02545	113.99	0.3899
17.74	0.02900	123.39	0.4173
19.19	0.03438	133.07	0.4437
20.63	0.04005	143.00	0.4689
22.08	0.04603	153.00	0.4928
23.48	0.05199	163.14	0.5161
25.43	0.06038	173.66	0.5391
27.86	0.07062	184.47	0.5607
30.22	0.08051	195.56	0.5801
32.54	0.09014	206.93	0.6009
34.80	0.09938	218.43	0.6171
37.03	0.1085	229.97	0.6373
39.24	0.1176	241.57	0.6552
41.43	0.1264	253.24	0.6726
43.62	0.1355	262.43	0.6836
46.93	0.1491	269.16	0.6958
51.29	0.1668	275.88	0.7028
55.54	0.1836	282.62	0.7111
59.77	0.2000	289.37	0.7187
63.88	0.2158	296.05	0.7257
67.90	0.2314	297.27	0.7266
71.85	0.2466	300.17	0.7297
75.71	0.2613	300.23	0.7289
82.09	0.2849	301.88	0.7307
87.50	0.3044	303.06	0.7329
92.39	0.3215		

Table 2 Experimental heat capacity of the hydrated composite "CaCl$_2$·2.04H$_2$O–silica gel" in J K^{-1} g^{-1}

T/K	C_p^o	T/K	C_p^o
14.05	0.01786	110.38	0.4637
15.47	0.02268	118.17	0.4933
16.86	0.02794	125.71	0.5209
18.2	0.03328	133.52	0.5483
19.53	0.03929	142.7	0.5790
21.18	0.04702	153.19	0.6128
23.05	0.05627	163.96	0.6460
24.98	0.06616	175.01	0.6795
27.42	0.07882	186.33	0.7111
30.29	0.09379	197.94	0.7409
33.19	0.1091	209.82	0.7731
36.01	0.1240	221.89	0.8057
38.68	0.1382	232.99	0.8390
41.97	0.1556	243.15	0.8665
45.92	0.1761	253.32	0.8944
49.84	0.1963	261.99	0.9146
54.13	0.2179	266.66	0.9294
58.79	0.2405	270.47	0.9381
63.45	0.2625	271.37	0.9405
68.16	0.2843	271.7	0.9380
72.9	0.3062	274.62	0.9465
77.67	0.3278	276.04	0.9505
81.7	0.3463	279.28	0.9574
85.62	0.3639	286.42	0.9746
89.12	0.3788	295.92	0.9930
92.72	0.3938	298.72	0.9998
96.36	0.4088	301.5	1.0068
102.25	0.4321		

Fig. 2 Heat capacity of composites CaCl$_2$–SiO$_2$ (*black circles*) and CaCl$_2$–H$_2$O–SiO$_2$ (*open circles*) at low temperatures

Fig. 1 Heat capacity of composites CaCl$_2$–SiO$_2$ (*black circles*) and CaCl$_2$–H$_2$O–SiO$_2$ (*open circles*) in a wide temperature range. *Open square* corresponds to heat capacity of CaCl$_2$–SiO$_2$ system at T = 314 K measured in [13]

The value of heat capacity 0.73 J K^{-1} g^{-1} measured by DSC method in [14] at T = 314 K for the anhydrous sample is also shown. It agrees with the present data within

the limits of error of DSC method. This is the only value from the earlier data on the similar sample that can be presented for comparison as those were measured at larger water content (3–7 mol H$_2$O per 1 mol CaCl$_2$) and higher temperatures (308–378 K). For none of the two samples was there any transition or thermal anomaly.

At very low temperatures (T < 13 K), experimental values of heat capacity of sample II were found to be equal to zero (Fig. 2). Similar phenomenon was observed at studying the heat capacity of coordination compound nickel (II) nitrate with 4-amine-1,2,4-triazole [15].

We assumed this effect to be due to the total absorption of helium by the sample. For sample I, this effect was not observed, but the dispersion of experimental points sufficiently increased in this temperature interval. This could be also associated with a partial sorption/desorption of helium. Therefore, all the thermodynamic calculations were made on the basis of experimental points obtained at T > 15 K.

To calculate the thermodynamic parameters, the obtained experimental data were extrapolated to the origin following the Debay law and smoothed using spline functions. The values of calorimetric entropy $S_{298}^0 - S_0^0$ and enthalpy increment $\Delta H_{298}^0 - \Delta H_0^0$ were derived by integration of the complete curve $C_p(T)$. The smoothed values at some selected temperatures are listed in Tables 3 and 4. The standard deviation of experimental C_p-values from the smoothed curve is equal to 0.7% at temperatures T < 30 K and 0.15% at 30 < T < 300 K.

For convenience of practical calculations, the experimental curves were also approximated by the following analytical expression

$$C_p(T) = A + BT + CT^2 + DT^3 + F\sqrt{T} + G\ln(T) \qquad (1)$$

Appropriate fitting coefficients are presented in Table 5. The standard deviation of experimental points from the so calculated curve for composite I was 0.8% at 15 < T < 30 K and 0.3% at 30 < T < 300 K. For composite II, these values, respectively, are 1.3 and 0.26% in the mentioned temperature intervals.

Table 3 Heat capacity, calorimetric entropy, and enthalpy of the anhydrous composite "CaCl$_2$–silica gel", $C_p^o(T)$, $S^o(T) - S^o(0)$ in J K^{-1} g^{-1}, $H^o(T) - H^o(0)$ in J g^{-1}, respectively

T/K	$C_p^o(T)$	$S^o(T) - S^o(0)$	$H^o(T) - H^o(0)$
14.97	0.01925	0.006415	0.07201
15	0.01938	0.006461	0.07268
16	0.02307	0.007831	0.09393
17	0.02662	0.009336	0.1188
18	0.03020	0.01096	0.1472
19	0.03390	0.01269	0.1792
20	0.03773	0.01453	0.2150
25	0.05842	0.02514	0.4547
30	0.07958	0.03766	0.7999
35	0.1003	0.05149	1.250
40	0.1208	0.06622	1.803
45	0.1412	0.08163	2.458
50	0.1615	0.09757	3.215
60	0.2011	0.1305	5.029
70	0.2396	0.1644	7.233
80	0.2773	0.1989	9.819
90	0.3131	0.2337	12.77
100	0.3466	0.2684	16.07
120	0.4076	0.3371	23.63
140	0.4615	0.4041	32.33
160	0.5092	0.4689	42.05
180	0.5517	0.5314	52.67
200	0.5884	0.5914	64.07
220	0.6213	0.6491	76.17
240	0.6527	0.7045	88.92
260	0.6815	0.7579	102.3
280	0.7074	0.8093	116.2
298.15	0.7277 ± 0.0030	0.8544 ± 0.0030	129.2 ± 0.5
300	0.7296	0.8589	130.5
303.06	0.7328	0.8663	132.8

Table 4 Heat capacity, calorimetric entropy, and enthalpy of the hydrated composite "CaCl$_2\cdot2.04H_2O$–silica gel", $C_p^o(T)$, $S^o(T) - S^o(0)$ in J K^{-1} g^{-1}, $H^o(T) - H^o(0)$ in J g^{-1}, respectively

T/K	$C_p^o(T)$	$S^o(T) - S^o(0)$	$H^o(T) - H^o(0)$
14.05	0.01752	0.00584	0.06154
15	0.02109	0.007101	0.07987
16	0.02491	0.008584	0.1029
17	0.02885	0.01021	0.1297
18	0.03294	0.01198	0.1606
19	0.03721	0.01387	0.1957
20	0.04166	0.01589	0.2351
25	0.06586	0.02773	0.5027
30	0.09186	0.04203	0.8966
35	0.1184	0.05818	1.422
40	0.1449	0.07572	2.081
45	0.1711	0.09431	2.871
50	0.1967	0.1137	3.791
60	0.2462	0.1539	6.007
70	0.2933	0.1955	8.706
80	0.3387	0.2376	11.87
90	0.3821	0.2800	15.47
100	0.4233	0.3224	19.50
120	0.5001	0.4065	28.75
140	0.5700	0.4889	39.46
160	0.6338	0.5693	51.51
180	0.6927	0.6474	64.78
200	0.7484	0.7233	79.19
220	0.8032	0.7972	94.71
240	0.8576	0.8694	111.3
260	0.9100	0.9401	129.0
280	0.9589	1.0094	147.7
298.15	1.0009 ± 0.0040	1.0709 ± 0.0040	165.5 ± 0.6
300	1.0051	1.0771	167.3
301.5	1.0086	1.0821	168.9

Useful comparisons can be made at the standard temperature 298.15 K. The experimental heat capacity of the anhydrous composite at 298.15 K is $C_p(I) = 0.7277 \pm 0.0030$ J g^{-1} K^{-1} (see Table 3). The dry composite consists of 64.3% of SiO$_2$ and 35.7% of CaCl$_2$. The heat capacity of confined salt can be calculated as $[C_p(I) - \alpha_1 C_p(SiO_2)]/\alpha_2$ where α_1 and α_2 are the weight fractions of the silica ($\alpha_1 = 0.643$) and the salt ($\alpha_2 = 0.357$). The value of the heat capacity of the silica KSK, $C_p(SiO_2) = 0.7850 \pm 0.0030$ J g^{-1} K^{-1} was obtained in our special experiments and will be published elsewhere. The calculated effective heat capacity of the confined salt $C_p(CaCl_2) = 0.624 \pm 0.005$ J g^{-1} K^{-1}. To compare it with the heat capacity of bulk salt, one can use the data of Kelley and Moore [16] in the temperature range of 52.6–295.1 K. The heat capacity at standard temperature

Table 5 Coefficients of Eq. (1) which ensure the best fit to the experimental C_p-curves

Sample	A	$B \times 10^3$	$C \times 10^6$	$D \times 10^{-10}$	F	G
I	0.02019	6.160	−15.4629	163.532	0	−0.0332
II	0.08872	−4.301	2.43605	−2.03538	0.2183	−0.3134

calculated by the data extrapolation is $C_p(298.15)$(bulk CaCl$_2$) = 0.6537 J g^{-1} K^{-1}. This C_p-value is sufficiently larger than the effective heat capacity of the confined salt (Fig. 3). Usually, the heat capacity of dispersed substance is larger than that of bulk material. In our case, the reduction of heat capacity of the confined salt may result from the strong chemical interaction between the confined salt and the host silica [10, 11].
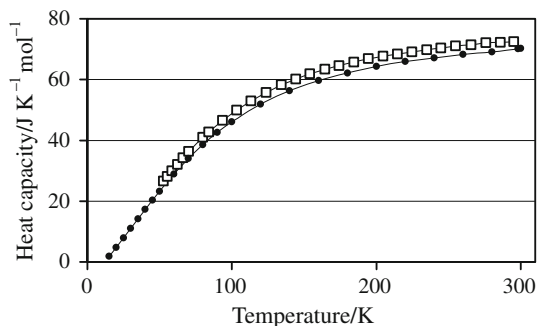
Fig. 3 Heat capacity of calcium chloride: *open squares*—the data for bulk salt [15], *black circles*—calculated values for dispersed salt

Similar estimations can be made for the hydrated composite "CaCl$_2$·2.04H$_2$O–silica gel". As the content of water in composite II was found to be more than 2 mol per 1 mol CaCl$_2$, it is assumed that the sample contains a quantity of tetrahydrate CaCl$_2$·4H$_2$O. In this case, one gram of hydrated composite consists of 0.575 g SiO$_2$, 0.415 g CaCl$_2$·2H$_2$O, and 0.010 g CaCl$_2$·4H$_2$O. Using the data on the heat capacity of CaCl$_2$ dihydrate and tetrahydrate [17], one can calculate the heat capacity of bulk sample with the composition of sample II C_p (bulk) = 0.948 J g^{-1} K^{-1}. This value is significantly smaller that the experimental one at 298.15 K C_{p298}^0 = 1.001 J g^{-1} K^{-1} (Table 4), hence, the heat capacity of the dispersed dihydrate is larger than that of the bulk one. The heat capacity of the dispersed dihydrate can be estimated as 1.29 J g^{-1} K^{-1} by making reasonable assumption that the contribution of the silica can be calculated from our unpublished results and that of CaCl$_2$·4H$_2$O—from its bulk heat capacity, 1.35 J g^{-1} K^{-1} [17]. This estimated value is 0.12 J g^{-1} K^{-1} larger than the heat capacity of the bulk dihydrate, 1.17 J g^{-1} K^{-1} [16]. This difference can be attributed to the enhancement of the water mobility in the dispersed hydrate as compared with the bulk one.

The analysis of the solid-state ^{2}H NMR line shape [18] showed that the temperature of the entire transformation of the solid to liquid-like NMR signal (T_{NMR} = 453 K) is in good correspondence with the melting point for the bulk dihydrate (T_m = 449 K [17]). For the dispersed dihydrate, this transformation occurs in a much broader temperature range, and the solid-like signal vanishes at T_{NMR} = 323 K that is much lower than the melting temperature of the dispersed dihydrate (T_m = 397 K communicated privately by A. V. Gubar). Hence, water molecules are more mobile in the dispersed dihydrate, and this mobility is not connected with the hydrate melting. This enhanced molecular mobility of water may be the reason for the increase in the heat capacity of the hydrated composite found in this article.

Table 6 Effective heat capacity of molecular H$_2$O in the hydrated composite in J K^{-1} mol^{-1}

T/K	C_p	T/K	C_p
15	0.6396	120	23.10
16	0.7290	130	24.96
17	0.8599	140	26.80
18	1.012	150	28.62
19	1.176	160	30.40
20	1.348	170	32.16
22	1.712	180	33.97
24	2.107	190	35.87
26	2.542	200	37.87
28	3.017	210	39.99
30	3.526	220	42.20
35	4.891	230	44.43
40	6.287	240	46.68
45	7.630	250	48.95
50	8.907	260	51.21
60	11.31	270	53.42
70	13.47	280	55.60
80	15.46	290	57.81
90	17.39	298.15	59.66
100	19.32	300	60.09
110	21.23		
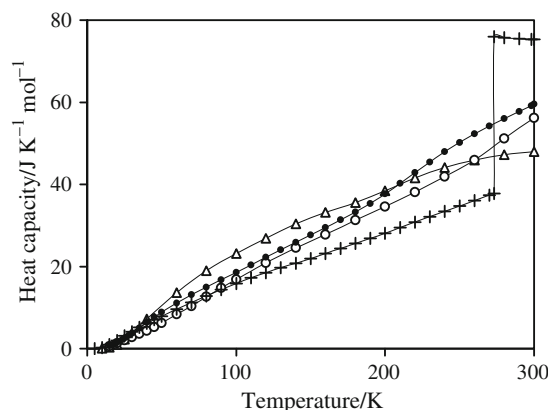
Fig. 4 Apparent heat capacity of molecular water in dispersed CaCl$_2$·2H$_2$O (*black circles*), analcime (*open triangles*), paranatrolite (*open circles*), and heat capacity of bulk H$_2$O (*plus signs*)

To single out the heat capacity $C_{p,m}^0(T)$ associated only with water in the hydrated composite, we calculated this value as the difference between the smoothed curves $C_{p,m}^0(T)$ of hydrated and anhydrous composites (Table 6). The accuracy of these values can be estimated as 4% at 15 K, 2% at 25 K, and 1% at 150–300 K. The effective heat capacity of confined water is a gradually increasing function of temperature (Fig. 4). It displays no phase transitions in the studied range of temperature and depends

mainly on the molecular mobility of water. This mobility in the bulk hydrate $CaCl_2 \cdot 2H_2O$ was analyzed in [20]: the translational modes of water were observed below 50 meV, the wagging, twisting, and rocking modes were found between 50 and 100 meV, while the deformation vibrations are active above ca. 200 meV. The QENS and INS spectra of the bulk dihydrate are typical of a solid with well-defined crystallographic positions for the water molecules [19], whereas the spectra for the dispersed hydrate display broad bands characteristic of more disordered substance [20].

The effective heat capacity of water in the hydrated composite was found to be close to that for mineral zeolites containing molecular water—analcime $NaAlSi_2O_6 \cdot H_2O$ [21] and paranatrolite $Na_2Al_2Si_3O_{10} \cdot 3H_2O$ [22]— and sufficiently differs from that for bulk water and ice (Fig. 4). The value of $C_{p,m}^0(T)$ is larger than that of the heat capacity of bulk ice and is significantly smaller that that of liquid water. Hence, the water molecules in the salt dihydrate are more mobile than in the bulk ice.

Conclusions

The heat capacities of the composite "$CaCl_2$–silica gel" in the anhydrous and hydrated states were measured over the temperature range of 6–300 K with the low temperature vacuum adiabatic calorimeter. Analytical expressions describing the temperature dependence of the composite heat capacities were derived. The heat capacity of anhydrous (hydrated) composite differs from those calculated as a linear addition of the corresponding values for the silica gel and the bulk calcium chloride (its dihydrate) taken with appropriate weight coefficients. As a result of the confinement, the C_p-value at 298.15 K reduced for the dispersed salt by 5% and increased for the dispersed dihydrate by 10%. The latter can be attributed to the enhancement of the water mobility in the dispersed hydrate as compared with the bulk one. The effective heat capacity of molecular water contained in the composite was calculated as a difference of the heat capacities of the anhydrous and hydrated samples. It appeared to be close to the heat capacity of water in zeolites analcime and paranatrolite and sufficiently larger than that of the heat capacity of a bulk ice.

References

1. Aristov YuI, Tokarev MM, Cacciola G, Restuccia G. Selective water sorbents for multiple applications: 1. $CaCl_2$ confined in mesopores of the silica gel: sorption properties. React Kinet Catal Lett. 1996;59:325–34.

2. Aristov YuI. New composite adsorbents "a salt in a porous matrix": designing sorption properties, In: Wong TW, editor. "Handbook of zeolites: structure, properties and applications". New York: Nova Science Publishers Inc.; 2009, Chapter 18, pp. 495–521.

3. Ştefănescu O, Davidescu C, Ştefănescu M, Stoia M. Preparation of FexOy/SiO2 nanocomposites by thermal decomposition of some carboxylate precursors formed inside the silica matrix. J Therm Anal Calorim. 2009;97:203–8.

4. Zou DQ, Yoshida H. Size effect of silica nanoparticles on thermal decomposition of PMMA. J Therm Anal Calorim. 2010;99:21–6.

5. Bai HY, Luo YL, Jin D, Sun JR. Particle size and interfacial effect on the specific heat of nanocrystalline Fe. J Appl Phys. 1996;79:361–4.

6. Herr U, Geigl M, Samwer K. Debye temperature of nanocrystalline $Zr_{1-X}Al_X$ solid solutions with different grain sizes. Philos Mag A. 1998;77:641–52.

7. Childress JR, Chien CL, Zhou MJ, Sheng P. Lattice softening in nanometer-size iron particles. Phys Rev B. 1991;44:11689–96.

8. Koops GEJ, Pattyn H, Vantomme A, Nauwelaerts S, Venegas R. Extreme lowering of the Debye temperature of Sn nanoclusters embedded in thermally grown SiO_2 by low-lying vibrational surface modes. Phys Rev B. 2004;70:235410–6.

9. Zhao SJ, Wang SQ, Cheng DY, Ye HQ. Three distinctive melting mechanisms in isolated nanoparticles. J Phys Chem B. 2001;105:12857–60.

10. Rossouw CJ, Donnelly SE. Superheating of small solid-argon bubbles in aluminum. Phys Rev Lett. 1985;55:2960–3.

11. Nanver LK, Weyer G, Deutch BI. Precipitation of β-tin in Sn implanted silicon. Phys Status Solidi A. 1980;61:K29–34.

12. Olsson J, Jernqvist Å, Aly G. Thermophysical properties of aqueous NaOH–H_2O solutions at high concentrations. Int J Thermophys. 1997;18:779–93.

13. Bessergenev VG, Kovalevskaya YuA, Paukov IE, Starikov MA, Opperman H, Reichelt W. Thermodynamic properties of $MnMoO_4$ and $Mn_2Mo_3O_8$. J Chem Thermodyn. 1992;24:85–98.

14. Aristov YuI, Tokarev MM, Cacciola G, Restuccia G. Properties of the system "calcium chloride–water" confined in pores of the silica gel: specific heat, thermal conductivity. Russ J Phys Chem. 1997;71:327–30.

15. Bessergenev VG, Kovalevskaya YuA, Lavrenova LG, Paukov IE. Low temperature heat capacity of the coordination compound nickel(II) nitrate with 4-amine-1,2,4-triazole at temperatures from 11 to 317 K. J Therm Anal Calorim. 2004;75:331–6.

16. Kelley KK, Moore GE. The specific heat at low temperatures of anhydrous chlorides of calcium, iron, magnesium and manganese. J Am Chem Soc. 1943;65:1264–7.

17. Meisingset KK, Grønvold F. Thermodynamic properties and phase transitions of salt hydrates between 270 and 400 K. IV. $CaCl_2 \cdot 6H_2O$, $CaCl_2 \cdot 4H_2O$, $CaCl_2 \cdot 2H_2O$, and $FeCl_3 \cdot 6H_2O$. J Chem Thermodyn. 1986;18:159–73.

18. Kolokolov DI, Stepanov AG, Glaznev IS, Aristov YuI, Jobic H. Water dynamics in bulk and dispersed in silica $CaCl_2$ hydrates studied by ^2H NMR. J Phys Chem C. 2008;112:12853–60.

19. Plazanet M, Glaznev IS, Stepanov AG, Aristov YuI, Jobic H. Dynamics of hydrated water in $CaCl_2$ complexes. Chem Phys Lett. 2006;419:111–4.

20. Kolokolov DI, Stepanov AG, Glaznev IS, Aristov YuI, Plazanet M, Jobic H. Water dynamics in bulk and dispersed in silica $CaCl_2$ hydrates studied by neutron scattering methods. Microporous Mesoporous Mater. 2009;125:46–50.

21. Johnson GK, Flotow HE, O'Hare PAG, Wise WS. Thermodynamic studies of zeolites: analcime and dehydrated analcime. Am Mineral. 1982;67:736–48.

22. Paukov IE, Moroz NK, Kovalevskaya YuA, Belitsky IA. Low-temperature thermodynamic properties of disordered zeolites of the natrolite group. Phys Chem Miner. 2002;29:300–6.